Nig. J. Pure & Appl. Sci. Vol. 32 (Issue 1, 2019)
ISSN 0794-0378

www.njpas.com.ng

https://doi.org/10.6084/m9.figshare.12276518 https://doi.org/10.7910/DVN/C0PQYU

EVALUATION OF TEMPERATURE DISTRIBUTIONS DURING MICROWAVE ABLATION OF EX VIVO BOVINE LIVER USING TWO TYPES OF ANTENNAS

Ibitoye A.Z.[1]*, Nwoye E.O.,[2] Saseyi A.O.,[1] Adeneye S.O.,[1] Adedokun M.B.[3] and Aweda M. A.[1]

[1]Department of Radiation Biology and Radiotherapy, College of Medicine, University of Lagos, Nigeria
[2]Department of Biomedical Engineering, College of Medicine, University of Lagos, Nigeria
[3]Department of Physics, University of Lagos, Nigeria

ABSTRACT

Introduction: Temperature distributions during microwave ablation are dependent on the antenna types, antenna geometry, tissue properties, input power and ablation. All these factors can significantly affect coagulation region, ablation length, ablation diameter, aspect ratio, backward heating (comic effect), and degree of necrosis. Temperature distributions during microwave ablation procedures determine the effectiveness of ablating tumour in tissue.

Objective: The aim of this study is to evaluate temperature distributions during microwave ablation using sleeved and dual slot antennas.

Materials and Methods: In this study, sleeved and dual slot antennas were designed using COMSOL MULTIPHYSICS software version 4.4. Temperature distributions were analyzed at 10 mm and 20 mm from the antennas' surfaces. Dual-slot and sleeved antennas were fabricated from 0.085' 50 Ω semi-rigid coaxial cable to conform to numerical simulation. The antennas were applied on *ex vivo* bovine liver. Thermometer probes were placed at 10 mm and 20 mm from the antennas' surfaces with the input powers set at 30, 50 and 80 W for 300 s. Before each ablation, initial temperature was recorded whereas subsequent measurements were recorded at 50 s intervals. Numerical simulation and experimental obtained data were analyzed and compared using the student's t-test statistical tool.

Results: The findings in this study showed that, temperatures produced at the two points of measurements by the sleeved antenna were greater than that of the dual-slot antenna in simulation and experimental procedures. Also, there was no significant difference between simulation and experimentally results for dual-slot antenna and sleeved antenna ($p = 0.25$).

Conclusion: In conclusion, the sleeved antenna has the potential to ablate a tumour faster above the tumoricidal temperatures at the same position than the dual-slot antenna.

Keywords: Microwave ablation; temperature distribution; dual-slot antenna; Comsol, Multiphysics; sleeved antenna

Introduction

Cancer is one of the most prevalent and complex global diseases worldwide according to the International Association of Cancer Registries, IACR (Ferlay *et al*. 2014). It is also a multifactorial and constantly evolving disease. Inappropriately, conventional treatments, such as radiotherapy and chemotherapy, have limited effectiveness in its treatment. Alternative cancer-specific and cost-effective treatment modalities are needed to complement these established techniques. Thermal

Corresponding Author: A. Z. Ibitoye* Department of Radiation Biology and Radiotherapy, College of Medicine of the University of Lagos, PMB 12003, Idi-Araba, Lagos State, Nigeria.
Phone: +2348028374385; Email: azibitoye@cmul.edu.ng

therapies such as radiofrequency ablation, high-intensity focused-ultrasound, cryoablation have been suggested as an alternative and a complement to existing techniques in the management of cancer (Habash *et al*. 2010; Brace 2011b).

In recent times, microwave ablation offers several advantages like the ability to ablate different tissues, cost-effectiveness and better localisation of heat energy makes it a choice over other forms of thermal therapies (Ahmed *et al*., 2011; Brace, 2011b). Frequencies of 915 MHz and 2.45 GHz are typically used clinically for microwave thermal ablation (Brace, 2009). Saccomandi and colleagues recently reported that ablation of the liver with a frequency of 2.45 GHz is more remarkable in performance than using a frequency of 915 MHz (Saccomandi *et al*., 2015). The performance of an antenna for microwave ablation has also been reported to be frequency dependent (Sawicki *et al*., 2017).

Microwave can cause oscillation of polar molecules to elevate temperatures in the tissue surrounding the antenna (applicator) at a very short time leading to tissue necrosis (Simon *et al*., 2006). The energy deposited during microwave ablation is proportional to the applied frequency, ablation duration and applied power. The degree of tissue necrosis is mostly affected by the heat distribution in the tissue, the type of antenna used, and biological tissue properties. Many antennas like slot, sleeved, choked, tri-axial and helical antennas have been proposed for use in microwave ablation thermal therapy. Their properties have been extensively reviewed in the literature (Bertram *et al*., 2006, Lubner *et al*., 2010; Brace, 2011b)

Apart from frequency, antenna geometries such as slot size, slot number, slot position and the addition of a metallic sleeve play significant roles on ablated diameter, backward heating along antenna shaft and the sphericity index of the ablated tissues (Brace, 2011a; Ibitoye *et al*., 2018). To study the performance of a good antenna, numerical simulation is mostly employed to understand the interaction of microwave radiation with biological tissues. Theoretical modelling has been playing significant roles in the design and optimization of antennas by serving as a quick, convenient and inexpensive tool to evaluate specific absorption rate (SAR), temperature, thermal dose and tissue damaged (necrosis) patterns. (Bertram *et al*., 2006; Prakash, 2010)

Heat transfer and electromagnetic propagation in tissue are best modelled using Pennes' bioheat equation and Maxwell's set of equations respectively (Hand 2008; Prakash 2010). The combination of these equations has proven to be an essential tool to predict electric field, temperature and microwave energy distributions in biological tissue (Prakash 2010, Ibitoye *et al*. 2018). In recent times, many researchers have used COMSOL MULTIPHYSICS, which is based on finite element methods (FEMs), to simulate and evaluate heating patterns of electromagnetic energy distributions in tissues during microwave ablation (Brace 2011b; Sarital *et al*. 2012; Ibitoye *et al*. 2015). Evaluation of temperature distribution during microwave thermal therapy is essential to provide an accurate

estimate of the region of coagulation necrosis. This will also help to reduce the risk of complications by sparing organs at risk in close proximity to the ablated region. As a result, reliable temperature information during clinical microwave ablation is desirable, for adequate treatment planning and effective delivery of the required thermal dose. This will also affect tumour control probability. Therefore, the aim of this study is to evaluate temperature distribution during microwave ablation of *ex vivo* bovine livers using numerical simulation and experimental methods with dual-slot and sleeved antennas.

MATERIALS AND METHOD

In this study, Comsol Multiphysics software version 4.4 (Stockholm, Sweden) was used to design and simulate the dual-slot and sleeved antennas' geometries, and also analyse electromagnetic and heat distribution in the ablated tissue. Temperature distributions were evaluated with this software by placing two thermometer probes at 10 mm and 20 mm away from the surface of the antenna to be within the ablating region (Figure 1). The antennas were fabricated from RG405 semi-rigid coaxial cable (Pasternack Enterprise Inc, Los Angeles, CA). A 2.45 GHz Sairem solid-state microwave generator (Neyron - Cedex, France) was used to generate a microwave signal. Bovine livers were obtained from the government approved abattoir for the experimental procedures. Tissue temperatures during experimental validation were recorded with a 4-Channel Data logging thermometer (SPER Scientific, Scottsdale) at 50 s intervals.

Simulation Procedure

Dual-slot and sleeved (dual-slot with a floating metallic sleeve) antennas were simulated with Comsol Multiphysics software version 4.4 which was based on the finite element methods (FEM). The software was used to design, simulate and compute temperature distributions in the liver. Radiofrequency and heat modules in the software were adopted to study Maxwell's and Pennes' bio-heat equations respectively (Hand, 2006). The geometries of the antennas were also modelled according to the specifications previously described extensively (Ibitoye *et al*. 2015). Liver dielectric properties were taken from literature and pre-defined values in the software (Hasgall *et al*., 2015). During the modelling, tissue was considered to be homogenous in a 2-D cylindrical symmetry with the antennas inserted into the cylindrically shaped liver to reduce computational time. Temperatures were measured at 10 and 20 mm from the antenna surface and at 10 mm from the antenna tip. Temperature versus time graphs at 50 s interval was plotted.

Experimental Validation

Ablations were performed on the *ex vivo* bovine liver obtained from government approved abattoir. Dual-slot and sleeved antennas were fabricated from a 50 Ω 0.087' RG 405/U semi-rigid coaxial cables to conform to the antennas specifications as described in the simulation. The two probes of the thermometer, P1 and P2, were inserted and placed parallel to the antenna at 10 and 20 mm to quantify

temperature in real-time during ablation (Figure 1). The input powers from the microwave generator were set at 30, 50 and 80 W for a duration of 300 s each. Initial temperatures before ablation of each liver were recorded. Subsequently, temperatures were measured and recorded in the real-time during ablation procedures at 50 s interval. The results obtained from both antennas were analysed using student t-test statistical method for comparing temperature distributions between the dual-slot antenna and sleeved antenna.

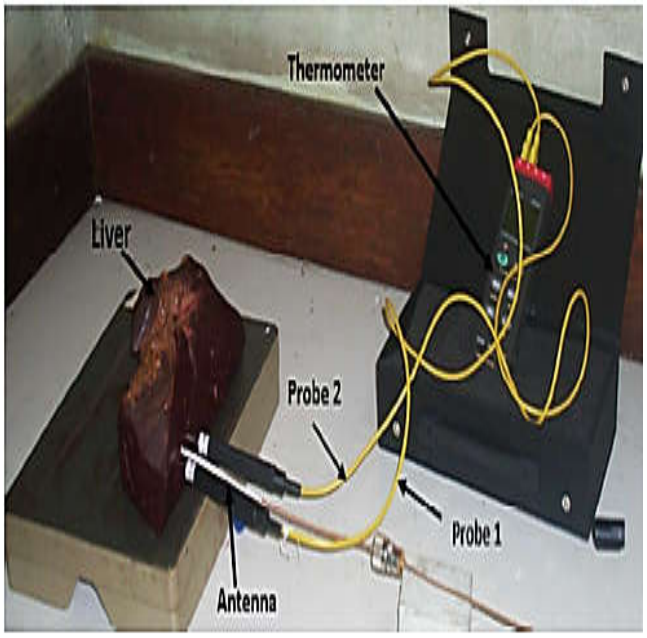

Figure 1: Experimental setup

RESULTS

Simulation results of temperature versus ablation durations are shown in Figures 1 and Table1 while experimental validation results are presented in Figure 3 for dual-slot antenna and sleeved antenna. Mean initial temperature before ablation began was 29.1±1.9 °C.

Fig. 2 is the 2-D isothermal contours of temperature distributions in the ablated liver. Temperature decreases from the antenna surface outward with sleeved antenna localised temperature distribution more than for dual-slot antenna. Temperature contours produced by the sleeved antenna were more spherical compared to those produced by the dual-slot antenna. In Table 1, when the input power was 30 W, the maximum temperatures recorded at 10 mm and 20 mm for the dual-slot antenna were 65.6 °C and 39.4 °C respectively while 76.6 °C and 41.0 °C for the sleeved antenna with $p = 0.005$ and 0.008 respectively. Also, in Table 1 when the input power was 50 W, the maximum temperatures recorded at points 10 and 20 mm for the dual-slot antenna were 87.1°C and 43.3 °C respectively while 105.3 °C and 43.4 °C were measured respectively for the sleeved antenna. Additionally, when the input power was set at 80 W, the maximum temperatures recorded at 10 and 20 mm for the dual-slot antenna were 119.3 °C and 49.4 °C respectively while for sleeved antenna 148.4 °C and 53.7 °C were measured respectively. There was also a significant difference between the temperature distributions produced by the sleeved and dual-slot antennas at 10 mm and 20 mm ($p = 0.01$). In Figure 3, the temperature measured during the ablation using sleeved antenna is greater than that of the dual-slot antenna by 28.2% and 7.6% at 10 mm and 20 mm respectively when the input power was set at 30 W. In the same figure, when the input power was 50 W, the average temperature measured during the ablation using sleeved antenna is greater than that of the dual-slot antenna by 7.7% and 15.4% at 10 mm and 20 mm respectively. In

addition, the average temperature measured during the ablation using sleeved antenna is greater than that of the dual-slot antenna by 10.3% and 4.7% at 10 mm and 20 mm respectively when the input power was 80 W. According to Table 4, the average temperature measured with the application of the sleeved antenna is greater than the dual-slot antenna. Temperature distributions were significantly difference between the two antennas used in this study at 10 mm ($p = 0.001$) and 20 mm ($p = 0.01$) from the surface of the antennas. Figure 4 shows sample of ablated liver with three distinguish ablation zones: charring zone, coagulation zone and congestion zone.

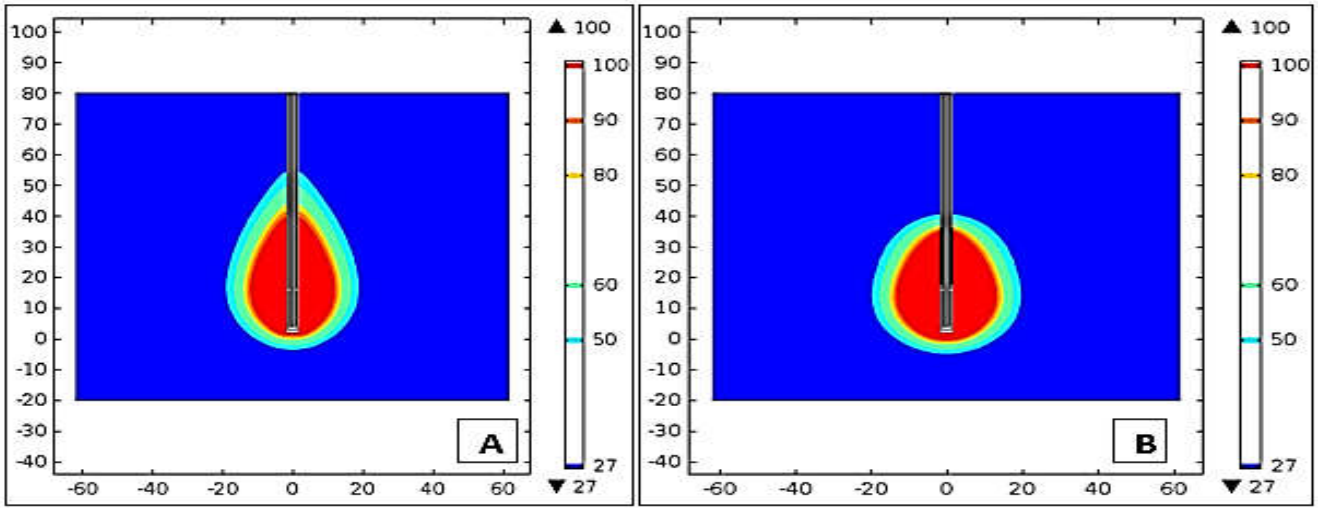

Figure 2: Simulation sample of temperature distributions using (A) dual-slot antenna and (B) sleeved antenna with the applied power of 80 W for 300 s

Table1: Temperature versus ablation duration with an input power of 30 W, 50 W and 80 W using (A) dual-slot antenna and (B) sleeved antenna.

Ablation Duration (s)	Power = 30 W				Power = 60 W				Power = 80 W			
	Probe 1 (°C)		Probe 2 (°C)		Probe 1 (°C)		Probe 2 (°C)		Probe 1 (°C)		Probe 2 (°C)	
	DSA	SA	DSA	SA	DSA	SA	DSA	SA	DSA	SA	DSA	SA
0	27.0	27.0	27.0	27.0	27.0	27.0	27.0	27.0	27.0	27.0	27.0	27.0
50	42.0	47.0	31.0	30.5	42.0	47.0	31.0	30.5	50.0	58.0	31.6	32.5
100	55.5	64.9	34.6	33.6	55.5	64.9	34.6	33.6	70.9	85.8	35.9	37.5
150	66.7	79.4	38.0	36.5	66.7	79.4	38.0	36.5	88.1	108.4	39.8	42.1
200	75.4	90.5	41.0	39.1	75.4	90.5	41.0	39.1	101.4	125.6	43.3	46.4
250	82.0	98.9	43.7	41.4	82.0	98.9	43.7	41.4	111.5	138.6	46.6	50.3
300	87.1	105.3	46.1	43.4	87.1	105.3	46.1	43.4	119.3	148.4	49.4	53.7
P-value	p = 0.005		p = 0.008		p = 0.005		p = 0.008		p = 0.005		p = 0.008	

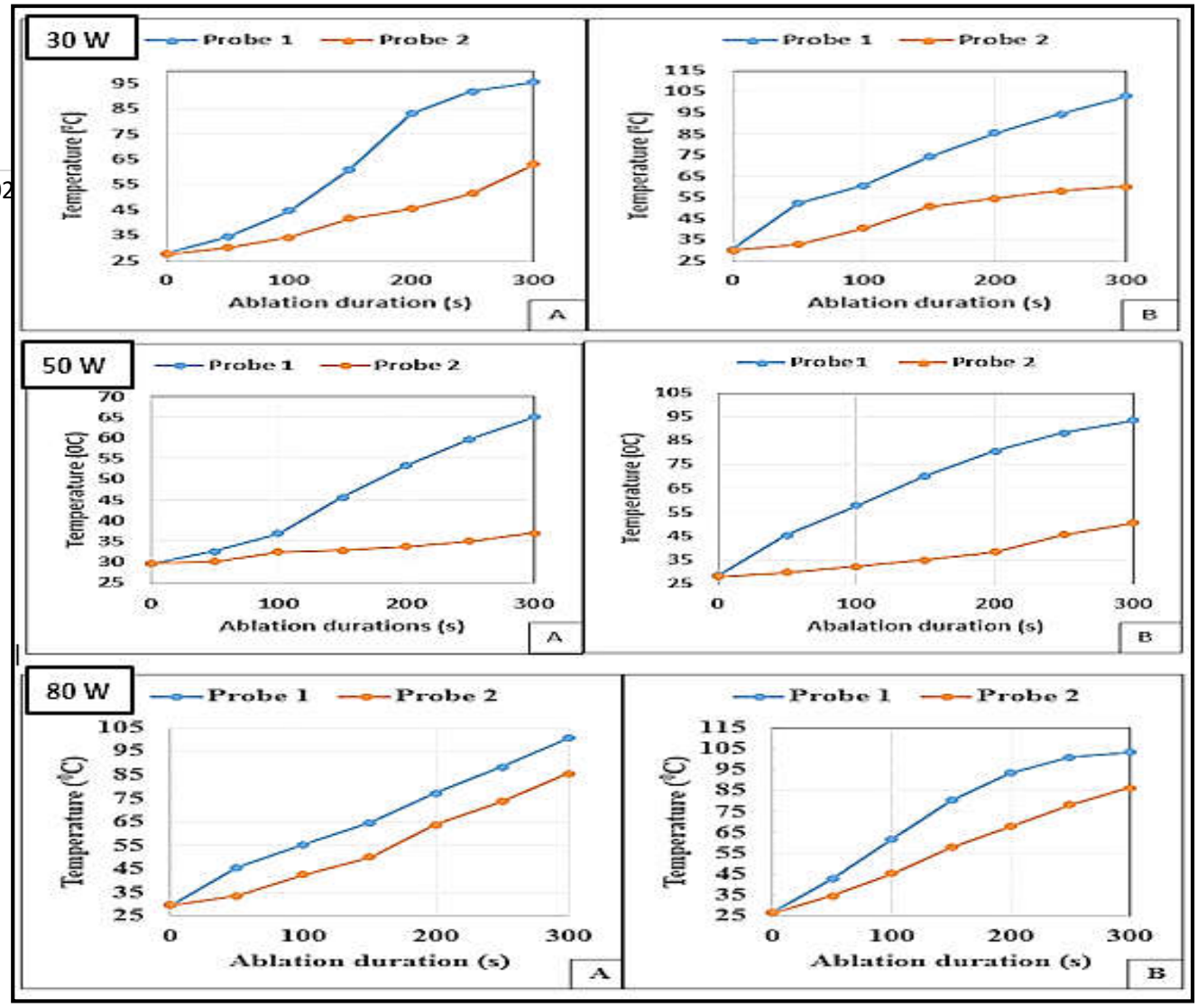

Figure 3: Temperature variation with time with (A) dual-slot and (B) sleeved antennas using 30, 50 and 80 W for 300 s at 10 and 20 mm from the surface of the antennas.

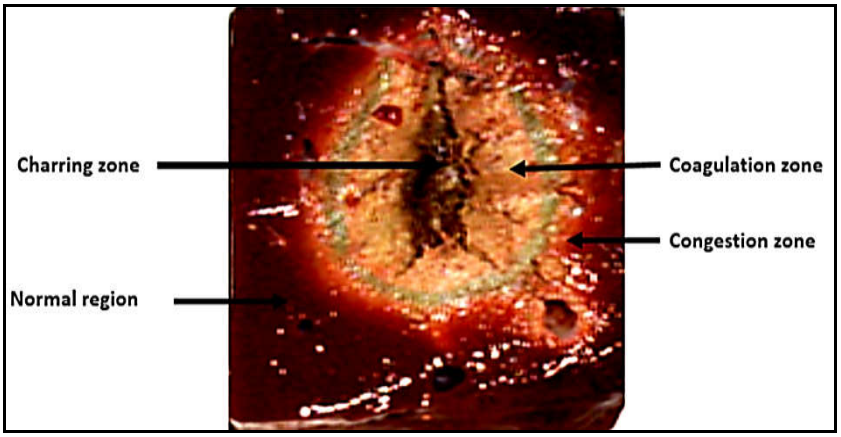

Figure 4: Sample of ablated ex-vivo bovine liver

Table 2: Mean ± standard deviation of temperatures at points 10 and 20 mm from the surface of dual-slot and sleeved antennas with input powers of 30, 50 and 80 W for 300 s

	Dual slot antenna		Sleeved antenna	
Time (s)	Probe 1 (°C)	Probe 2 (°C)	Probe 1 (°C)	Probe 2 (°C)
0.0	30.0±2.3	29.5±2.2	28.7±1.9	28.2±1.8
50.0	39.0±5.8	31.5±2.7	43.5±1.7	32.5±2.4
100.0	48.6±5.8	35.9±8.6	58.4±3.0	39.4±6.5
150.0	59.7±5.4	38.2±10.4	72.6±6.7	47.9±11.5
200.0	73.3±12.3	45.7±18.4	82.5±10.0	53.7±14.6
250.0	80.4±13.9	52.0±19.2	91.1±8.5	60.7±16.4
300.0	88.6±16.5	60.3±23.4	98.5±4.9	65.7±18.4

Discussion

This study presents temperature distributions during ablation procedures using a sleeved antenna and dual-slot antenna on *ex vivo* bovine liver. The applied power and ablation duration determine the value of the temperature measured at a particular point in ablated tissue (Hope *et al*. 2008). Antenna types and tissue properties also contributed to variation in temperature distribution in the ablation volume. The discrepancy in temperatures between simulated and experimentally values was found to be more pronounced when high input powers were applied for a longer duration. Also, complexity in liver properties used for the experimental validation is in contrast to the homogeneity assumption adopted during simulation procedures, hence results in variation in measured temperatures. The roles of numerical simulation in microwave ablation have been discussed extensively (Bertram *et al*. 2006; Prakash 2010). The outcome of this study is an indication that a simulation method is a valuable tool for predicting temperature distribution during microwave ablation technique. Temperatures measure decreases from the antenna surface outwards due to absorption and attenuation of the microwave energy by water molecules in the liver. On the pathologic inspection of the ablated liver, three zones of different degrees of ablation were noted. The inner zone appears charred, dark and brittle due to high temperatures around the antenna. The middle zone appeared pink with indications of coagulation necrosis and the outer appeared brighter at the boundary between the coagulated region and unaffected part with minimal temperature change as shown in Figure 4. These ablation zones have also been reported to vary with the applied power, ablation duration and distance

from the antenna surface (Gas, 2012). In this study, there was no significant difference between simulation and experimental results which is in agreement with the study by Deshazer *et al* that simulation procedure is suitable to predict tissue temperature when the antenna geometry is unknown (Deshazer *et al*., 2017).

Generally, sleeved antenna produced higher temperature distribution than dual-slot antenna as revealed in Table1. This is as a result of the inclusion of copper sleeve to reduce backward heating along the antenna leading to better localisation of microwave energy into the ablated tissue (Yang *et al*., 2006; Ibitoye *et al*., 2015). During microwave ablation, the temperature can exceed 100 °C depending on the ablation duration, applied power and antenna type (Brace, 2009). Above 100 °C, differences in measured temperature are minimal due to reduced water content as a result of vaporisation of tissue water content and change in the tissue relative permittivity and effective (Ji and Brace, 2011). Many researchers have focussed mostly on designing of suitable antennas to ablate large tumour volume, increase sphericity index and reduce backward heating along antenna shaft with little emphasis on the heat distribution (Yang *et al*. 2006; Bertram *et al*., 2006; Brace, 2011a; Sarital *et al*., 2012; Ibitoye *et al*., 2016). In this study, we have been able to quantify temperatures in real time at different locations using simulation and experimental validation methods. Antenna geometries play significant roles in power distribution, temperature distribution and the degree of coagulation necrosis as revealed in this study which is in agreement with Keangin *et al*., 2011.

A good understanding of temperature distribution during microwave ablation will be essential in the treatment planning of patients. Since the geometry of antenna plays significant roles in microwave power deposition during microwave ablation, choice of appropriate antenna for a particular treatment will determine the heat distribution pattern which will eventually affect the tumour ablation outcome. Although in vivo validation was not conducted, we expect similar results would be achieved with the use of these antennas and other variables such as applied input powers, ablation durations and accurate placement of the thermometer probes at distance 10 and 20 mm from the antennas surfaces.

CONCLUSION

This study presents temperature distributions in *ex vivo* bovine livers using computer simulation and experimental validation methods. The obtained results show that the measured temperatures in the *ex vivo* bovine liver with the sleeved antenna is higher than that of the dual-slot antenna. The study also revealed that no significant difference exists between temperatures measured during simulation and experimental procedures with both antennas. Conclusively, the sleeved antenna would be more appropriate for ablation of soft tissues where high temperature is desirable than the dual slot antenna which is mostly used clinically for the ablation of soft tissues.

Conflict of interest: None

REFERENCES

Ahmed. M., Brace. L C., Fred, T.L., and Goldberg, S.N. (2011). Principles of and advances in percutaneous ablation. *Radiology,* 258(2):251-269.

Bertram, J.M., Yang, D., Converse, M.C., Webster, G.J., and Mahvi, M.D. (2006). Antenna design for microwave hepatic ablation using an axisymmetric electromagnetic model. *Biomedical Engineering Online*. 5:15 doi:10.1186/1475-925X-5-15.

Brace, L.C. (2009). Microwave ablation technology: what every user should know. Current Problems in Diagnostic Radiology, 38: 61–67.

Brace, L.C. (2011a). Dual-slot antennas for microwave tissue heating: parametric design, analysis and experimental validation. *Medical Physics*, 38:4232-4240.

Brace, L.C. (2011b). Microwave Tissue Ablation: Biophysics, Technology and Applications. *Critical Reviews in Biomedical Engineering,* 38(1): 65-78.

Deshazer, G., Prakash, P., Merck, D. and Haemmerich, D. (2017). Experimental measurement of microwave ablation heating pattern and comparison to computer simulations. *International Journal of Hyperthermia,* 33(1):74-82.

Ferlay, J., Soerjomataram, I., Dikshit, R., Eser, S., Mathers, C., Rebelo, M., Parkin, D.M., Forman, D., and Bray, F. (2015). Cancer incidence and mortality worldwide: Sources, methods and major patterns in GLOBOCAN 2012. *International Journal of Cancer*, 136: 359-386.

Gas, P. (2012). Temperature distribution of human tissue in interstitial microwave hyperthermia. *Przeglad Elektrotechniczny (Electrical Review),* 88(7):144-146.

Habash, R.W.Y., Bansal, R. Krewski, D. and Alhafid, H.T. (2007). Thermal therapy, Part III: ablation techniques. *Critical Reviews in Biomedical Engineering,* 35:37–121.

Hand, J. W. (2008). Modelling the interaction of electromagnetic fields (10 MHz–10 GHz) with the human body: methods and applications. Physics in Medicine and Biology, 53(16), R243–R286. https://doi.org/10.1088/0031-9155/53/16/R01

Hasgall, P.A., Di Gennaro, F., Baumgartner, C., Neufeld, E., Gosselin. M.C., Payne, D., Klingenböck, A., and Kuster, N. (2018). "IT'IS Database for thermal and electromagnetic parameters of biological tissues," Version 4.0, May 15, 2018, DOI: 10.13099/VIP21000-04-0. itis.swiss/database.

Hope, W.W., Schmelzer, M.T., Newcomb, L.W., Heath, J.J., Lincourt, E.A., Norton, J.H., Heniford, T.B., and Lanitti, A.D. (2008). Guidelines for power and time variables for microwave ablation in a porcine liver. *Journal of Gastrointestinal Surgery,* 12:463-467.

Ibitoye, A.Z., Orotoye, T., Nwoye, E.O., and Aweda, M.A. (2018). Analysis of Efficiency of Different Antennas for Microwave Ablation using Simulation and Experimental Methods. *Egyptian Journal of Basic Applied Sciences,* 5(1): 24-30.

Ibitoye, A.Z., Nwoye, E.O., Aweda, M.A., Oremosu A.A., Anunobi C.C., and Akanmu O.N. (2015). Optimization of dual slot antenna using floating metallic sleeve for microwave ablation. *Medical Engineering and Physics*, 37:384–391.

Ji, Z., and Brace, L.C. (2011). Expanded modeling of temperature-dependent dielectric properties for microwave thermal ablation. Physics in Medicine Biology, 56(16): 5249–5264. doi:10.1088/0031-9155/56/16/011.

Keangin, P., Rattanadecho, P., and Wessapan, T. (2011). An analysis of heat transfer in liver tissue during microwave ablation using single and double slot antenna. *International Communications in Heat and Mass Transfer*, 38: 757-766.

Lubner, M.G., Brace, L.C., Henshaw, J.L., and Lee, F.T. (2010). Microwave tumor ablation: mechanism of action, clinical results, and devices. *Journal of Vascular and Interventional Radiology*, 21: 192–203.

Prakash, P. (2010). Theoretical modeling for hepatic microwave ablation. *Open Biomedical Engineering Journal*, 4:27–38.

Saccomandi, P., Schena,E., Massaroni, C., Fong, Y., Grasso, R.F., Giurazza, F., Zobel, B.B., Buy, X., Palussiere, J., and Cazzato, R.L. (2015). Temperature monitoring during microwave ablation in *ex vivo* porcine livers. *European Journal of Surgical Oncology,* 41(12): 1699-16705.

Sarita, M, Marwaha, A., and Marhawa, S. (2012). Finite element analysis of optimizing antenna for microwave coagulation therapy. *Journal of Engineering, Science and Technology,* 7:462–70.

Sawicki, F.J., Shea, D.J., Behdad, N., and Hagness, C.S. (2017). The impact of frequency on the performance of microwave ablation. *International Journal of Hyperthermia,* 33: 61-68.

Simon, C.J., Dupuy, D.E., and Mayo-Smith, W.W. (2005). Microwave ablation: Principles and applications. *RadioGraphic*, 25:69–83.

Yang, D., Converse, M.C., Mahvi, M.D., and Webster, G.J. (2006). Measurement and analysis of tissue temperature during microwave liver ablation. *IEEE Translational Biomedical Engineering*, 54(1): 150-155.